Simulation of a latex balloon with a hydrogen generation system

Vasco Miguel Campos da Gama Teles Cepêda

Instituto Superior Técnico, Universidade de Lisboa, Lisboa, Portugal

September 2020

Abstract

Nowadays, given their physical properties and cheaper technologies, stratospheric balloons are widely used in most of the environmental monitoring missions. Nevertheless, controlling their altitude is challenging, especially when dealing with a stratosphere where winds can reach 100 Km/h and temperatures may achieve -90°C. Finding a way to control their movement becomes essential. The main objective is to control the volume and the total mass of the balloon, and force it to find favorable wind streams in order to ensure it will always remain within a certain region. The most recent solutions are distinguished not only by the control method but also by the type of gas and balloons that are used. Moving towards a more academic environment, where cost and time are factors to consider, the laboratory is a valid starting point for the development of a prototype: a latex balloon equipped with a hydrogen production system, generated through the hydrolysis reaction of calcium hydride. Nonetheless, to develop such prototype, pre-knowledge about the system's behaviour is crucial, in order to reduce costs and save time for the future project generations. Given this, a simulator for the total system is proposed. To study the hydrolysis reaction, a chemical reactor prototype was developed and tested before the appearance of the virus COVID-19. For the other subsystems, fluid mechanics and thermodynamic principles were applied, and a suitable group of equations was used to describe their behaviour. The final model was developed in *Matlab/Simulink* R2018a.

Keywords: stratospheric balloons, hydrogen, latex, calcium hydride, hydrolysis

1. Introduction

With an uncontrolled growth of the earth's population, global warming has become the issue of our time. High altitude monitoring systems have never played such an important role. Until now, drones were widely used for most of the environmental monitoring missions, but the problem is that they are quite limited in what concerns their flight autonomy. Stratospheric balloons appear to complement them: the idea is to use a balloon to work as their moving platform. Nonetheless, controlling a stratospheric balloon is challenging. Given the harsh conditions presented in stratosphere, the durability of these missions is highly affected by the duration of the flights. Finding a way to control the balloon's movement becomes an essential task.

1.1. Existing solutions

The most recent solutions are distinguished not only by the control mechanisms but also by the type of lift gas and balloons that are used. In the past few years, helium has been identified as an endangered element, as the lack of it and the challenges associated to its extraction are responsible for a serious market helium supply crisis [1]. In a transition to a more sustainable future, hydrogen has been the subject of a great deal of research and it does present a lot more advantages, specially for high altitude balloon applications. The biggest challenge associated with it is related to its storage, but many solutions have already overpass this disadvantage. Metal hydrides are chemical compounds which generate hydrogen through their hydrolysis reaction. Basically, when a metal reacts with hydrogen at really high pressure conditions, a metal hydride is formed and the possibility of storing hydrogen in powder form appears, thus eliminating the challenge usually associated to its storage. Nevertheless, within the extended universe of metal hydrides, most of them react violently with water and the others are really expensive. This work analyses the hydrolysis reaction of calcium hydride CaH_2. Regarding controlling mechanisms, very interesting ideas have been proposed in the past few years. Project Loon, for example, proposed three different solutions [2]. In the first one, altitude is decreased by pumping lift gas to a higher pressure storage chamber. To increase it, the gas is returned to the envelope. In the second solution, the balloon runs a fuel cell in reverse: to increase the altitude, H_2 is produced via electrolysis and sent back to the envelope; to decrease the altitude, hydrogen returns to the fuel cell, to generate electricity and water and once again re-

vert the process. In the third solution, half of the balloon is painted white and the other half black. Depending on the side of the balloon that is faced towards the sun, the gas will expand or contract and a change in the altitude will be applied. Regarding latex balloons, recently, a group of researchers showed that, by managing the lift gas mass and the system's total weight (by dropping ballast), they could extend their flight duration from 3 hours to several days and provide the possibility to achieve higher altitude variations [3].

1.2. Objectives and contributions

This work proposes a different solution: a latex balloon equipped with a hydrogen production system, generated from the hydrolysis of CaH_2. Fig. 1 schematizes the final prototype. It is composed by

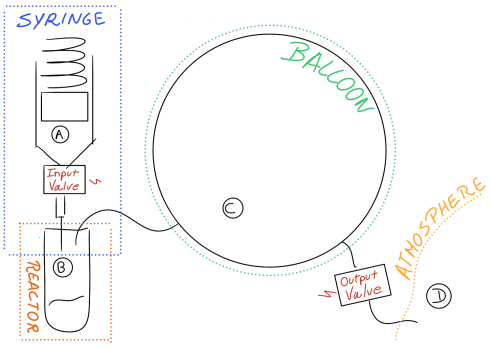

Figure 1: Proposed solution.

the **syringe subsystem** (●), responsible for injecting the necessary amount of water into the reactor; the **reactor subsystem** (●), where the hydrolysis occurs; the **balloon subsystem** (●), responsible for carrying all the components and finally, the **atmospheric subsystem** (●), used to simulate the atmospheric conditions.

Regarding its actuation mechanisms, these are also represented: one to control the mass of water (the **input valve**) (to produce H_2 and elevate the balloon) and a second one to release H_2 (the **output valve**). To develop this prototype is a very challenging task, as most of the parameters involved are difficult to be determined without carrying out some practical experiments. Given its practical complexity, and because of the pandemic, a computational model was developed in order to allow for future generations to predict the way the system would behave if its parameters were changed. This was the final goal of this project.

2. Theoretical modelling

This section presents the theoretical principles and physical assumptions that were considered for the modelling phase.

2.1. Syringe subsystem

Figure 2 schematizes the syringe subsystem.

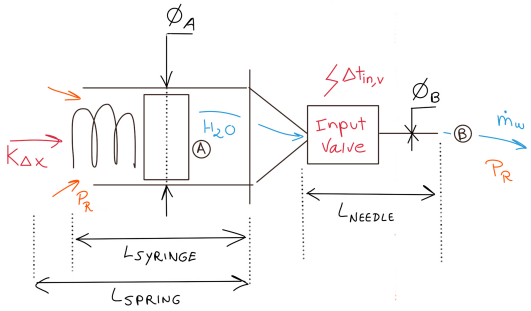

Figure 2: Syringe subsystem

It is governed by the transient *Bernoulli's* principle, applied between points A and B:

$$p_A + \rho_\omega g z_A + \frac{1}{2}\rho_\omega u_A^2 = p_B + \rho_\omega g z_B + \frac{1}{2}\rho_\omega u_B^2 + \rho_\omega \int_{x_A}^{x_B} \frac{du(x)}{dt} dx + \int_{x_A}^{x_B} f \frac{1}{2} \frac{L_s}{\phi_s(x)} \rho_\omega u(x)^2 dx \quad (1)$$

where, x and z represent the fluid's longitudinal and vertical coordinates, respectively, u the fluid's longitudinal velocity along the syringe's streamline (being $x = 0$ the plunger's position for the situation at which the spring is at its most contracted position), p and ρ_ω represent the fluid's pressure and density, respectively, L_s the streamline's length, g the acceleration of gravity, ϕ_s the syringe subsystem's diameter at a specific section, f the *Darcy* coefficient and $\rho_\omega \int_{x_A}^{x_B} \frac{du}{dt} dx$ represents the transient term. The following assumptions were made:

- Incompressible flow: $\rho_\omega = \text{cte}$;
- Flow rate continuity: $Q_\omega = \text{cte}$;
- Neglected velocity terms: $u_A \approx u_B \approx 0$;
- Neglected gravity term: $\rho_\omega g z_A \approx \rho_\omega g z_B$[1];
- Transient term simplification: $\rho_\omega \int_{x_A}^{x_B} \frac{du(x)}{dt} dx \approx \rho_\omega \frac{du_{needle}}{dt} L_{needle}$;
- Simplified loss term: $\int_{x_A}^{x_B} f \frac{1}{2} \frac{L_s}{\phi_s(x)} \rho_\omega u(x)^2 dx = f \frac{1}{2} \frac{L_{needle}}{\phi_B} \rho_\omega u_{needle}^2$;
- Laminar flow [4]: $f_{needle} \frac{1}{2} \frac{L_{needle}}{\phi_B} \rho_w u_{needle}^2 = \frac{32 \mu_\omega L_{needle} u_{needle}}{{\phi_B}^2}$, where μ_ω represents the water's dynamic viscosity and ϕ_B the diameter of the needle section;
- One dimensional flow;
- Syringe subsystem assumed to be well isolated

[1] in fig. 2, the system was represented horizontally (different from the way it would be placed in the prototype). Still, in the lab, it was noticed that gravity could be neglected, given the surface tension effects noticed at the tip of the needle.

and located inside the reactor subsystem: $p_A = p_R + \frac{F_{spring}}{A_{plunger}} = p_R + \frac{4k(L_{spring}-x)}{\pi\phi_A^2}$.

After making all of these assumptions, the water mass flow rate $\dot{m}_\omega$ may be computed by using the following expressions: $\frac{4k(L_{spring}-x)}{\pi\phi_A^2} = \rho_\omega \ddot{x}\frac{\phi_A^2}{\phi_B^2}L_{needle} + \frac{32\mu_\omega L_{needle}\dot{x}\phi_A^2}{\phi_B^4}$ (eq.(1) simplified) and $\dot{m}_\omega = \rho_\omega \frac{\dot{x}\pi\phi_A^2}{4}$ where $\ddot{x}$ represents the plunger's acceleration.

2.2. Reactor subsystem

Figure 3 schematizes the reactor subsystem.

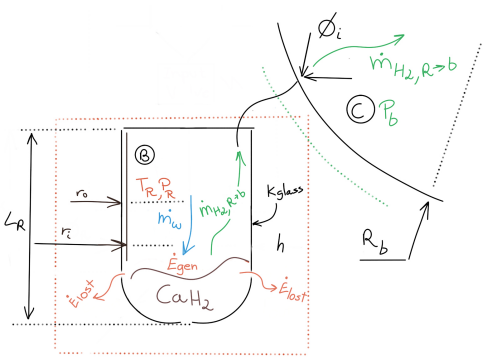

Figure 3: Reactor subsystem

In the reactor, H_2O reacts with CaH_2 to form H_2 and $Ca(OH)_2$ according to:

$$CaH_2(s) + 2H_20(l) \rightarrow Ca(OH)_2(aq) + 2H_2(g) + 183\ KJ \quad (2)$$

The following physical assumptions were made:
- Constant reactant purity;
- Deviated stoichiometry: with the laboratory experiments, it was noticed that, without the presence of a chemical catalyst, 4 to 6 times more water was needed to produce the theoretical amount of H_2.

At the laboratory (section 3), it was quite difficult to record the initial slope of the hydrogen curve, thus making it a lot more challenging to study the reaction in what concerns its kinetic rate. Due to the pandemic, the analysis of the reaction was conditioned by the type of results that were obtained until the date. Given this, by still trying to use the laboratory curves, a different approach was considered: hydrogen behaves as an ideal gas and the internal temperature of the reactor is obtained by using the well-known *Lumped capacitance method* [5]. The amount of hydrogen leaving the reactor is then obtained by using the *Bernoulli's* principle, this time applied between points B and C. Once water is added to the reactor, hydrogen is generated according to a specific transfer function (section 4.2). As hydrogen is generated, the reactor's internal density and temperature will change according to the next equations, respectively: $\frac{d}{dt}(\rho_{H_2,R}V_R) = \dot{m}_{H_2,gen}(\approx f(\dot{m}_\omega)^2) - \rho_{H_2,R}\frac{\pi\phi_i^2}{4}v_i$ (the mass balance of the system) and $\rho_{H_2,R}Cp_{H_2}V_R\frac{d}{dt}(T_R) = \dot{E}_{gen} - \dot{E}_{lost}$ (the lumped capacitance method approximation), where $\rho_{H_2,R}$ represents the reactor's internal density, V_R the reactor's fixed volume, $\dot{m}_{H_2,gen}$ the generated hydrogen mass flow rate, ϕ_i the diameter of the tube connecting the balloon to the reactor, v_i the hydrogen's velocity in this tube, Cp_{H_2} the hydrogen's heat capacity, T_R the reactor's internal temperature and $\dot{E}_{gen}$ and $\dot{E}_{lost}$ the generated and released energy powers, respectively. Regarding the last equation, $\dot{E}_{gen}$ is a function of the entalphy of reaction H_R (eq.(2)) and the amount of hydride that is being consumed, and $\dot{E}_{lost}$ is computed by: $\dot{E}_{lost} = \frac{T_R - T_{out}}{\Omega_T}L_R$, where L_R is the reactor's length, T_{out} is the outside temperature and Ω_T the total thermal resistance, calculated by using the reactor's equivalent thermal circuit: $\Omega_T = \frac{1}{2\pi r_o h} + \frac{ln\left(\frac{r_o}{r_i}\right)}{2\pi k_{glass}}$, where k_{glass} represents the glass thermal conductivity, h the convection coefficient, r_i the reactor's internal radius and r_o the reactor's external radius ($r_o = r_i + t_{glass}$). Finally, once pressure is known ($p_R = \rho_{H_2,R}R_{g,H_2}T_R$), $\dot{m}_{H_2,R\to b}$ (from the reactor to the balloon) is computed by using the simplified *Bernoulli* equation: $p_R = p_b + \frac{1}{2}\rho_{H_2,R}v_i^2$.

2.3. Balloon subsystem

Figure 4 schematizes the balloon subsystem.

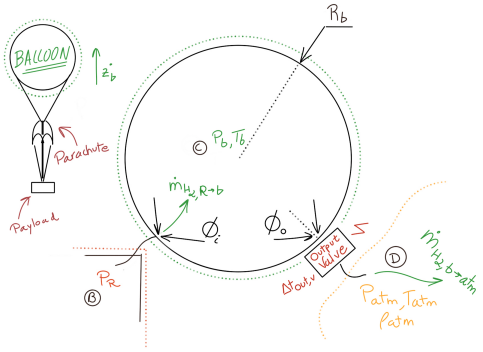

Figure 4: Balloon subsystem

The balloon's movement is governed by the *Archimedes* principle:

$$\sum F = m_{total}\frac{d\dot{z}_b}{dt} = \rho_{atm}V_b g - m_{total}g - \frac{1}{2}C_D A_b \rho_{atm}\frac{dz_b}{dt}\left|\frac{dz_b}{dt}\right| \quad (3)$$

where $\rho_{atm}V_b g$ and $\frac{1}{2}C_D A_b \rho_{atm}\frac{dz_b}{dt}\left|\frac{dz_b}{dt}\right|$ represent the buoyancy and drag forces, respectively. The

[2] see section 4.2

balloon was assumed to be spherical with a perfect deflation mechanism (meaning it will expand in the same way it may contract), and with a neglected temperature transient phenomena, i.e. $T_b \approx T_{atm}$. Besides this, hydrogen was also assumed to behave as an ideal gas, $p_b = \rho_{H_2,b} R_{g,H_2} T_b$. Finally, by being a latex balloon which is able of exchanging mass with its neighbouring environment, the way the balloon behaves is complemented with 3 additional equations:

- The *Mooney-Rivlin* equation [6]: $[p] = 2s_+ \frac{t_e^0}{r_b^0} \left(\frac{r_b^0}{R_b} - \left(\frac{r_b^0}{R_b} \right)^7 \right) \left(1 - \frac{s_-}{s_+} \left(\frac{R_b}{r_b^0} \right)^2 \right)$ where $[p]$ represents the over-pressure, $p_b - p_{atm}$, t_e^0 and r_b^0 represent the thickness and radius of the undeformed envelope, respectively, s_+ and s_- are elastic temperature linearly dependent constants and R_b is the current radius of the balloon.
- The mass balance: $\frac{d}{dt} \left(\frac{4\pi R_b^3 \rho_{H_2,b}}{3} \right) = \dot{m}_{H_2,R \to b} - \rho_{H_2,b} \frac{\pi \phi_o^2}{4} v_o$, where $\rho_{H_2,b}$ represents the balloon's internal density, ϕ_o represents the diameter of the outlet tube, v_o is the velocity of the gas exiting through this tube and $\dot{m}_{H_2,R \to b}$ the hydrogen input mass flow rate.
- The *Bernoulli's* equation, applied between points B and C, and C and D: $p_R = p_b + \frac{1}{2} \rho_{H_2,R} v_i^2$ and $p_b = p_{atm} + \frac{1}{2} \rho_{H_2,b} v_o^2$, respectively.

By merging all of these equations, one is able to solve for the radius of the balloon R_b at each instant of time and calculate the altitude of the balloon z_b for the same instant by using equation (3).

2.4. Atmosphere subsystem

To obtain the values for the atmospheric pressure, density and temperature, the ISA (International Standard Atmospheric) model was used [7]. The model provides average values of air pressure p_{atm}, air temperature T_{atm} and air density ρ_{atm} for each specific altitude z_b.

3. Studying the hydrolysis reaction

This chapter presents the chemical reactor prototype and analyses the hydrolysis reactions of CaH_2.

3.1. Chemical reactor prototype

Figure 5 presents the final installation.

A set composed of a syringe, the input valve, its respective needle, and a fixed lead metal mass is responsible for pressuring the water down (fig. 5(a)). Once actuated (order given by an *Arduino* code command), water droplets will fall and react with the chemical hydride (stored inside the reactor) to form hydrogen (fig. 5(b)). Once formed, temperature and pressure will increase, and the gas will be released through the hydrogen tube (fig. 5(a) in blue), towards the inverted beaker, in order to be measured (fig. 5(c)). For temperature, two thermocouples were placed as represented in fig. 5(b) and connected to an external multimeter: the first one to measure the reaction core temperature (placed inside the reactor); the second one to measure the temperature of the reactor's surface. This installation was developed with the goal of establishing an easy way to control the water mass flow rate. For this, it was used the *Arduino* represented in fig. 5(a) and a balance with a maximum precision of 0.001 g. Fig. 6 presents the results.

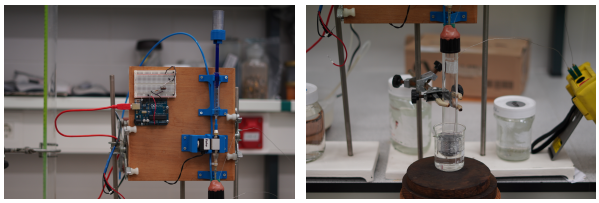

(a) Prototype front view (b) Reactor detailed view

(c) Beaker's entrance (d) Work station

Figure 5: Chemical reactor's prototype

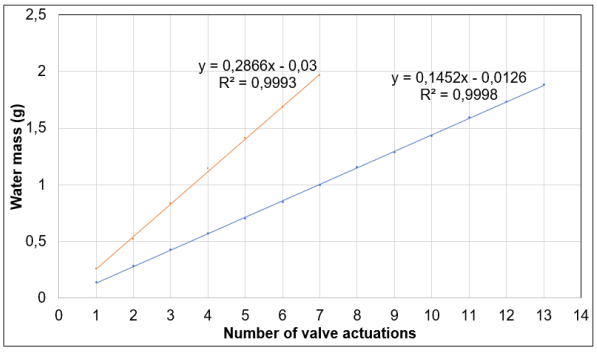

Figure 6: Water mass measured on the balance over time [g]. Orange curve ●: Actuation time = 190 ms. Blue curve ●: Actuation time = 80 ms.

In fig. 6, each mass point was recorded 20 seconds after the previous point. The following conclusions were taken:

- The water mass measured on the balance varied linearly with time. This allowed to confirm that the friction factor is always the same.
- To achieve the double of the rate, one would expect an opening time of 160 ms (2×80 ms), however, for that, it was necessary to increase the actuation period to 190 ms (fig. 6). Noticing this, before any

hydrolysis reaction, first it was ensured that the water mass flow rate would be the desired one.

3.2. Experimental results

After improving the quality of the installation, the hydrolysis reactions were tested. At first, H_2O and CaH_2 were mixed together in different amounts in order to study the effect of each one of the reactants in the hydrogen production (H_2O added in one single shot). Tab. 1 presents the initial conditions for the first three tests. The results are in fig. 7.

Table 1: Laboratorial "single-shot" tests conditions

Test	$\Delta t_{in,v}$[ms]	$m^0_{[CaH_2]}$[g][3]	$m^0_{H_2O}$[g]
1	80	0.232	≈ 0.1452
2	80	0.456	≈ 0.1452
3	190	0.225	≈ 0.2866

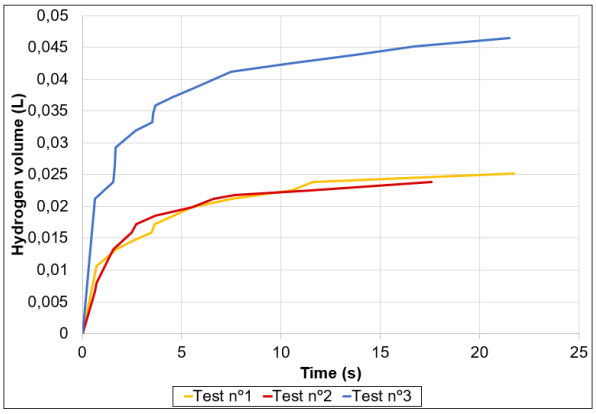

(a) Volume of hydrogen produced (L)

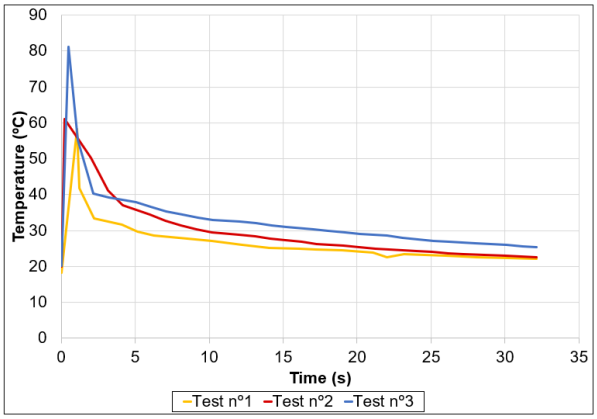

(b) Temperature responses (°C)

Figure 7: Hydrolysis reactions (tests n°1, 2 and 3)

The following conclusions were taken:

- When comparing the H_2 curves of tests n°1 and n°2, by doubling the initial mass of CaH_2 and maintain the initial amount of H_2O, no difference was noticed. This was expected: since water is the limiting reactant, an increase of the CaH_2 concentration will produce an almost null effect.

- By comparing tests n°1 and n°3, a huge difference in production of H_2 was noticed. Once again, this came to confirm the water reactant as being the main reaction controller. The volume of hydrogen varies linearly with the initial amount of water.

- The stoichiometric production ratio was never achieved. Take a look at test n°3: 0.225 grams of CaH_2 reacted with approximately 0.286 grams of water (water added in excess) to yield only about 0.05 liters of hydrogen (more or less 25% of the theoretical volume). In addition, water was added in excess. Theoretically, 0.225 grams of CaH_2 require more or less 0.194 grams of water to produce 0.225 liters of hydrogen. To produce this quantity, one would need 4 times more water than the amount that was added, i.e., 5 to 6 times more water than predicted. This result is explained by the poor dissolution of $Ca(OH)_2$. $Ca(OH)_2$ presents the very low solubility of 0.00173 g/cm^3 at 20°C. Moreover, its solubility decreases with temperature, which might be seen right now as a larger inconvenience, as the hydrolysis is highly exothermic. Due to all of this, it is natural that, for producing the stoichiometric quantity of hydrogen, one will need more or less 5 times more water than theoretically stated.

- In what regards the temperature curves (fig. 7(b)), these were very inconclusive. Hydrogen production varied linearly with water, but the same did not occur for the temperature. The inconsistency might however be explained by the lab conditions: the outside temperature was always varying; the amount of cold water used to refrigerate the reaction might have been slightly different for the different reactions; temperature was not measured exactly at the core of the reaction, and finally, the multimeter used to perform the readings did not have an enough sampling resolution to capture the real temperature growth.

To validate these results, a different test was performed. This time, instead of a making a "single-shot" test, water was added repeatedly on droplets form. An initial mass of 0.125 grams of pure CaH_2 was poured inside the test tube and within intervals of 20 seconds, a constant mass of approximately 0.0263 grams of water was added. Fig. 8 presents the results. With these results, 4 to 5 times more water was, once again, required to achieve the H_2 volume close to the stoichiometric one. In this reaction, 0.125 g of CaH_2 were poured inside the reactor, which theoretically, produce around 0.125 liters of H_2 when put together with 0.1075 g of H_2O. The reaction stabilized at t = 400 s, thus meaning that around 400/20 x 0.0263 g = 0.526 g of H_2O were

[3] reactant with a purity of 92%

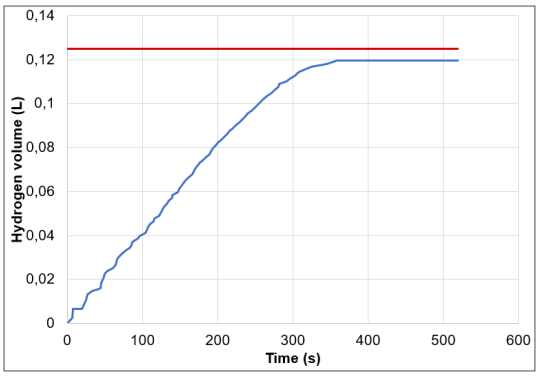

Figure 8: Hydrolysis reaction (test n°4): Red curve ●: theoretical limit for hydrogen production (according to equation (2)); Blue curve ●: actual volume of hydrogen produced

necessary. Still, after 400 s, the theoretical value was still not achieved, which is explained by the reactant's level of purity. With this new test, a new value of 88% was estimated. Since the results were not as good as expected, especially regarding temperature, it was considered the curves corresponding to tests n°1 and n°3 for the next phase (fig. 7(a)). Furthermore, it was assumed that water varied linearly with the actuation time and finally, given the results of fig.7(a), the volume of H_2 produced was also assumed to vary linearly with the initial amount of H_2O, and a transfer function was found for relating the two variables (section 4.2).

4. Simulator development and respective validation

This chapter focuses on the implementation aspects regarding each one of the subsystems. The different models were implemented in *Matlab/Simulink* R2018a. Most of the models here described try to simulate the behaviour of laboratory-scaled devices, as most of the practical results were obtained with a small reactor and syringe. Since no experiment included a practical latex balloon, an appropriate weather balloon was chosen and a final simulator for a latex balloon carrying a 10ml syringe and a 15cm-height reactor was developed. These dimensions and quantities might not seem realistic, but since it was not possible to measure the mass of all the other payload components and since the experiments were performed at the laboratorial scale, no other dimensions were assumed.

4.1. Syringe model

The model outputs a certain water mass flow rate $\dot{m}_\omega$ as a function of the reactor pressure p_R, the valve actuation time $\Delta t_{in,v}$ and a set of constant parameters. These are resumed in tab. 2. Fig. 9

Table 2: Syringe model parameters ($\delta_t = 0.001s$)[4]

Geometric properties		Fluid properties		System inputs[5]	
ϕ_A [m]:	0.0146	μ_ω [Pa.s]:	10^{-3}	p_R [Pa]:	101493
ϕ_B [m]:	0.0007	ρ_ω [Kg/m^3]:	1000		
L_{needle} [m]:	0.025				
$L_{syringe}$ [m]:	0.06				
k [N/m]:	20				

presents the results that were obtained for the case of a syringe smaller than the spring[6].

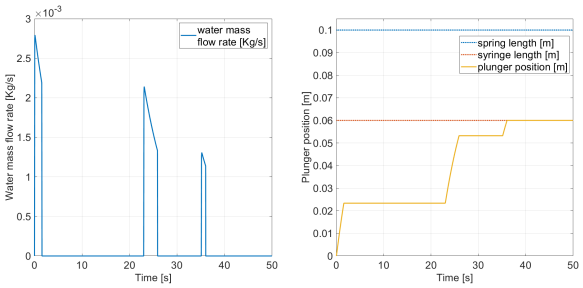

(a) $\dot{m}_\omega$ (Kg/s) (b) x (m)

Figure 9: Syringe model validation: results for the case at which ($L_{spring} > L_{syringe}$).

The results confirm that the model was well implemented: it was expected for the syringe's plunger to reach its final position x (fig. 9(b)) before the water mass flow rate turns zero (fig. 9(a)). The model was designed to work for every possible situation.

4.2. Chemical reaction parameterization

Since the practical experiments displayed very poor results, for computing $V_{H_2,gen}$, the laboratorial curve corresponding to test n°3 was used (fig. 7(a)). Its hydrogen volume response was imported to *Matlab* together with its input signal (constant water mass flow rate during a period of 160ms) and the toolbox *"ident"* was used to obtain a transfer function for relating the water mass flow rate $\dot{m}_\omega$ with the amount of hydrogen produced $V_{H_2,gen}$ (in liters). The best fitting results were obtained with this function:

$$G(s) = \frac{50.1218s^3 + 115.6012s^2 + 24.7381s + 0.6803}{s^4 + 1.0931s^3 + 0.1636s^2 + 0.0039s} \quad (4)$$

4.3. Reactor model

For the reactor, the model outputs a certain H_2 input mass flow rate $\dot{m}_{H_2,R\rightarrow b}$ as a function of the balloon's pressure p_b, the hydrogen generation mass flow rate $\dot{m}_{H_2,gen}$, and a set of other parameters. These are resumed in tab. 3. For its validation, the

[4] δ_t represents the sampling time for all the subsystems
[5] neglected for this case (syringe placed inside the reactor)
[6] valve opened when $\dot{m}_\omega \neq 0$
[7] assumed constant for this case

Table 3: Reactor model parameters ($\delta_t = 0.00001s$)

System inputs[7]		Physical properties		Geometric properties		Other parameters	
p_b [Pa]:	101493	k_{glass} [W/(m.K)]:	0.67	r_i [m]:	0.015	Cp_{H_2} [J/(Kg.K)]:	14.5
		h [W/(m^2.K)]:	100	L_R [m]:	0.15	H_R [KJ/mol$_{[CaH_2]}$]:	183
		T_{out} [K]:	288.19	ϕ_i [m]:	0.001	V_M [dm^3/mol]:	22.4
				t_{glass} [m]:	0.002		

laboratory conditions of test n°3 were replicated. Fig. 10 presents the results.

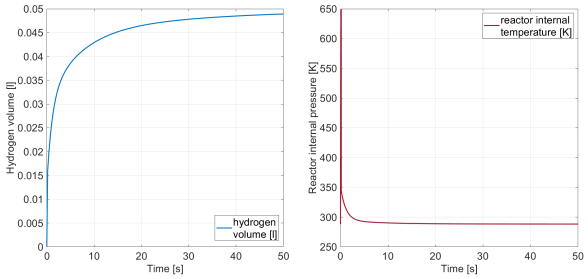

(a) $V_{H_2,gen}$ (l)

(b) T_R (K)

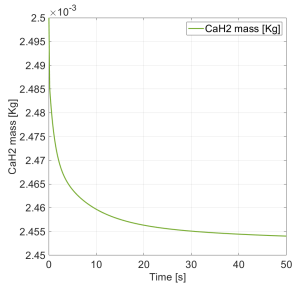

(c) $m_{[CaH_2]}$ (Kg)

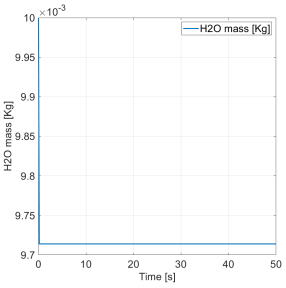

(d) m_ω (Kg)

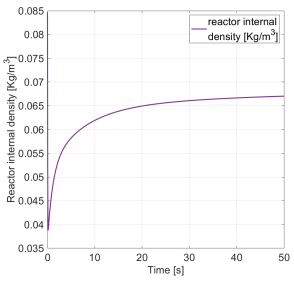

(e) $\rho_{H_2,R}$ (Kg/m^3)

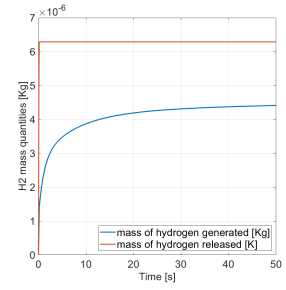

(f) $m_{H_2,gen}$, $m_{H_2,R\rightarrow b}$ (Kg)

Figure 10: Reactor model validation: replication of test n°3

As it happened in test n°3 (fig. 7(a)), 0.286 grams of water were added to the reactor during a period of 160 ms (fig. 10(d)) and only 0.05 grams of CaH_2 were consumed (5 to 6 times less than stoichiometrically expected) (fig. 10(c)). With these quantities, 0.05 liters of hydrogen were produced (the same result as in test n°3, thus proving the model is well implemented). Regarding the results displayed in fig. 10(b), the internal temperature of the reactor has increased to 650 K (an increase of approximately 350°C). One would say this value is extremely high when compared to the one obtained in the laboratory (fig. 7(b)), however one must consider once again all the laboratory conditions: temperature was not measured at the core of the reaction; the multimeter had a shorter sampling resolution than desired. All of these combined with the approximations that were assumed make the comparison between the simulation and laboratory results more challenging. Finally, to confirm that the model was correctly implemented, the hydrogen mass balance was analysed: the mass of hydrogen inside the reactor at the beginning ($\rho^0_{H_2,R}V_R$) plus the amount that was generated ($m_{H_2,gen}$ at t = 50s) must be equal to the amount that was released ($m_{H_2,R\rightarrow b}$ at t = 50s) plus the amount that was kept inside the reactor ($\rho_{H_2,R}V_R$ at t = 50s). By looking at the different instants, figures 10(e) and 10(f) confirm this result.

4.4. Balloon model

For the balloon, the model outputs the balloon's radius R_b and altitude z_b as a function of the atmospheric conditions (p_{atm}, ρ_{atm} and T_{atm}), the input and output H_2 mass flow rates ($\dot{m}_{H_2,R\rightarrow b}$ and $\dot{m}_{H_2,b\rightarrow atm}$) and a set of constant parameters. Since no practical experiment was performed (already explained at the beginning of chap. 4), it was assumed a normal latex weather balloon. Its specifications are represented in tab. 4. Tab. 5 resumes the chosen parameters, where m_{rest} represents the mass of the unknown components (batteries, supports, tubes, etc...), $\rho^0_{H_2,b}V^0_b$ the initial H_2 mass and C_D the balloon's drag coefficient.

Table 4: Weather balloon specifications (TA 200)[8]

TA 200 type: weather balloon specifications	
Barely inflated radius: $r^0_b[m]$	0.275
Weight ($m_e[kg]$)	0.2
Parachute's mass ($m_{pch}[kg]$)	0.07
Recommended payload mass ($m_{pl}[kg]$)	0.250
Launch radius ($R^0_b[m]$)	0.558
Bursting radius ($R_{b,burst}[m]$)	1.5
Bursting altitude ($z_{b,burst}[m]$)	21200

Table 5: Balloon model parameters ($\delta_t = 0.001s$)

System inputs[8]		Total mass		Geometric prop.		Other param	
$\dot{m}_{H_2,R\rightarrow b}$ [Kg/s]:	3.72×10^{-4}	m_{pch} [Kg]:	0.07	ϕ_o [m]:	0.03	t^0_e/r^0_b:	0.008
T_{atm} [K]:	288.19	m_e [Kg]:	0.2			r^0_b [m]:	0.275
p_{atm} [Pa]:	101493	m_{rest} [Kg]:	0.2			s_+ [bar]:	3
ρ_{atm} [Kg/m^3]:	1.2271	m^0_ω [Kg]:	0.01			s_- [bar]:	-0.3
		$m^0_{[CaH_2]}$ [Kg]:	0.0025			C_D	0.47
		$\rho^0_{H_2,b}V^0_b$ [Kg]:	0.063				

[8] assumed constant for this case

To validate, a simple test was performed, in order to check for the presence of a typical *Mooney-Rivlin* pressure curve. For this, despite the values that were considered for the system's total mass, here, the entire mass was assumed to be zero. Tab. 6 presents the initial conditions for the simulation and fig. 11 presents its most important results.

Table 6: Balloon test initial conditions

Balloon test initial conditions	
T_b^0 [K]:	288.19
p_b^0 [Pa]:	101493
$\rho_{H_2,b}^0$ [Kg/m^3]:	0.0847
R_b^0 [m]:	0.275 [8]
z_b^0 [m]:	0

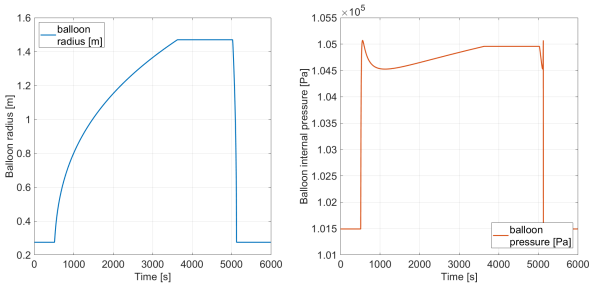

(a) R_b (m) (b) p_b (Pa)

Figure 11: Balloon model validation

Since the model considers constant atmospheric conditions and zero mass (only for this simulation), it was possible to start the simulation with the balloon barely inflated (tab. 4) and check for the *Mooney-Rivlin* pressure curve [6]. At the pressure peak, the size ratio R_b/r_b^0 was close to 1.5 and the over-pressure between the internal and external pressures was equal to 35 mbar, thus proving the model was correctly implemented [6] (recall that the atmospheric pressure was considered constant for this model in particular (tab. 5)). Furthermore, once the balloon stopped being inflated, since the model does not consider the porous properties of normal latex balloons and since the atmospheric conditions were always the same, its properties remained constant. Finally, at the end, the balloon was deflated, and a *Mooney-Rivlin* curve was also noticed because the same equation was considered for the deflation process. The difference in time that was noticed is explained by the diameter that was considered for the balloon's outlet neck, ϕ_o (tab. 5).

4.5. Atmospheric model

In order to check for the influence of the atmospheric properties, a simple simulink block was develop to implement the ISA model [7]. For a proper validation, the previous balloon model was also considered. The difference between this model and the one explained in the previous chapter lies on values that were considered for its parameters: this time, the full mass of the entire system was included (tab. 5) and it was allowed for the atmospheric conditions to change. For its validation, the balloon started its flight with its recommended launch radius (tab. 4) and the simulation has stopped once the balloon achieved an hovering condition. Tab. 7 presents the initial conditions. The results are represented in fig. 12.

Table 7: Atmosphere test initial conditions

Atmosphere and balloon test initial conditions	
T_b^0, T_{atm}^0 [K]:	288.19
p_{atm}^0 [Pa]:	101493
p_b^0 [Pa]:	104785
$\rho_{H_2,b}^0$ [Kg/m^3]:	0.0875
R_b^0 [m]:	0.558
ρ_{atm}^0 [Kg/m^3]:	1.227
z_b^0 [m]:	0

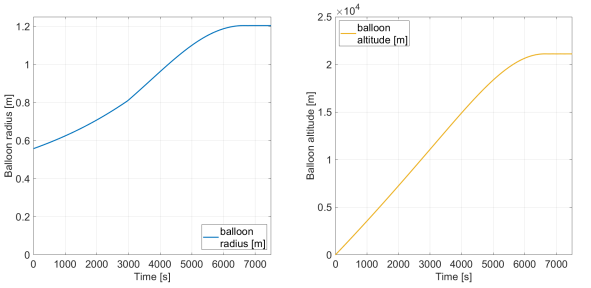

(a) R_b (m) (b) z_b (m)

Figure 12: Balloon + Atmospheric model validation

The results prove the model is well implemented. During the simulation, no additional hydrogen mass has entered or left the balloon. Given its sufficiently high initial radius and constant change in atmospheric conditions, the balloon actually starts to expand until an hovering condition is achieved. This is demonstrated in figures 12(a) and 12(b): the balloon radius expanded from 0.588 m to 1.2 m and it reached an altitude close 21500 m, approximately, where it kept still because of the balance of forces. Despite being close to reality, some aspects were noticed regarding the obtained results: in tab. 4, it is said the balloon will burst with a radius of 1.5 m at an altitude close to 21200 m. The balloon has reached this altitude with less 30 cm than expected. This might be explained by the approximations that were considered: hydrogen was assumed

to behave as an ideal gas; the *Mooney-Rivlin* is an approximation which might not perfectly represent this balloon's elastic deformation; the elastic coefficients (s_+ and s_-) used in the *Mooney-Rivlin* equation were kept constant during the entire simulation (due to lack of information); the ISA model might provide unreal results if compared with the conditions of the tests that were performed to define the balloon's specifications, etc. Still, the model behaves as pretended and the errors that were noticed might still be improved if more information is available in the future.

5. Latex balloon with a hydrogen generation system: final simulator

For the final simulator, all the previous models were merged together. The difference in the implementation was only one: the reactor and balloon subsystems were joined in order for their values to be computed exactly at the same time. Now, every system is connected with the others: the water mass flow rate $\dot{m}_\omega$ is given by the syringe model and used to compute the hydrogen volume generation rate (eq.(4)). Then, with this result, and by constantly receiving the pressure from the balloon p_b at any instant of time, the reactor model will output the amount of hydrogen that will enter the balloon $\dot{m}_{H_2,R\to b}$. At the same time, the balloon model interacts with the atmospheric model and depending on the amount of hydrogen received and released ($\dot{m}_{H_2,b\to atm}$), a certain altitude z_b will be achieved by the balloon (eq.(3)). For the total system validation, it was assumed the balloon was already floating at an altitude close to 21100 m. The initial conditions for the simulation are represented in tab. 8 and fig. 13 presents the results for some of the variables that were analysed. Regarding these final results, at $\approx$ 70s, the valve was actuated and the entire amount of water (fig. 13(f)) was used to provide an altitude variation of about 35 m (fig. 13(b)). With the results represented in figure 13(d), one might confirm that the model was well implemented. In the hydrolysis of test n°3 (fig. 7(a) and tab. 1), 0.286g of water were mixed with CaH_2 to yield 0.05 liters of H_2. In this case, 10g of water were released, and so therefore, one expected to obtain 1.74 liters, i.e., 0.150 g of H_2. Fig. 13(d) confirms this result. By comparing the results from figures 13(c) and 13(d), the amount that was generated $m_{H_2,gen}$ was almost equal to the amount that was released $m_{H_2,R\to b}$. In addition to this, the density inside the reactor was equal at the beginning and end of the simulation. These two results also prove the model was correctly implemented. Finally, at t $\approx$ 700s, a certain amount of H_2 was released (fig. 13(e)) and the balloon achieved an altitude close to its initial one (fig. 13(b)) with the same radius (the mass released was very little).

Table 8: Final test initial conditions

Final simulator initial conditions (test n°2)	
T_b^0, T_{atm}^0 [K]:	216.69
p_b^0 [Pa]:	$\approx$ 7842
p_R^0 [Pa]:	$\approx$ 7840
p_{atm}^0 [Pa]:	$\approx$ 4644
$\rho_{H_2,b}^0$ [Kg/m^3]:	$\approx$ 0.0087
$\rho_{H_2,R}^0$ [Kg/m^3]:	$\approx$ 0.0065
R_b^0 [m]:	$\approx$ 1.2041
ρ_{atm}^0 [Kg/m^3]:	$\approx$ 0.0747
$m_{[CaH_2]}^0$ [Kg]:	0.0025
$m_{[H_2O]}^0$ [Kg]:	0.01
v_i^0 [m/s]:	0
v_o^0 [m/s]:	0
$\dot{z}_b^0$ [m/s]:	$\approx$ 0.0074
z_b^0 [m]:	$\approx$ 21111

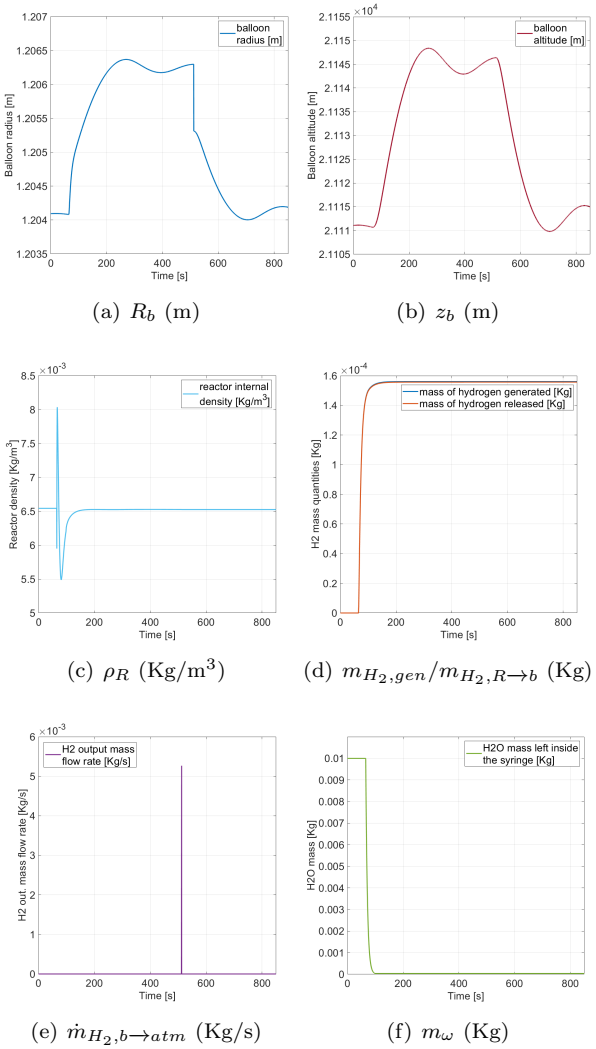

(a) R_b (m) (b) z_b (m)

(c) ρ_R (Kg/m^3) (d) $m_{H_2,gen}/m_{H_2,R\to b}$ (Kg)

(e) $\dot{m}_{H_2,b\to atm}$ (Kg/s) (f) m_ω (Kg)

Figure 13: Final model results

6. Conclusions

This work started with idea of building a physical prototype in the laboratory, but due to the pandemic, the final target was changed. Still, the model that was created helps to extract valid conclusions regarding the behaviour that the physical prototype would eventually display. The simulator allows to change specific parameters and check their effect on the total system's response. Regarding the results that were obtained, with an additional hydrogen quantity of 0.150g, the balloon's altitude has increased about 35m (fig. 13). Nevertheless, the amount that was generated was highly affected by the reactant available quantities and by the results obtained with the hydrolysis reaction (section 3). One noticed the reaction is actually very slow and that is probably because of the hydroxide's poor solubility. Practically, in all the experiments that were performed, 5 to 6 times more water was necessary to achieve the stoichiometric hydrogen production. The chemical prototype that was developed suits to achieve consistent constant water mass flow rates, but for the reaction, a lot of things should be improved.

For future work, it is suggested to study the hydrolysis more carefully. The rate of reaction is highly dependent on its core temperature. Unfortunately, it was quite hard to capture the temperature growth, and because of that the results were highly affected. It is suggested to measure the reaction's temperature closer to its core, or, in case of not being possible, one suggests the use of a multimeter with a higher sampling resolution. Furthermore, the efficiency of the process must be increased: one may use chemical catalysts to increase the rate of reaction, or in case CaH_2 presents bad results either way, other hydrides should be studied. Let's consider the perfect situation, where hydrogen is produced according to the stoichiometric ratio: with 10 g of water, the mass that would be generated would be something close to 1 g, 10 to 11 times more mass than the one generated in the final test that was performed (fig. 13). Furthermore, if the available payload space would allow for greater reactant quantities, this mass would be even higher, which would greatly increase the duration of the balloon's flight.

Regarding the model, some possible improvements are suggested. In the laboratory, a glass-reactor was used for the experiments, and because of this, the same was considered for the model. Nevertheless, the model does not consider the reactor sensitivity. If a certain differential pressure is achieved between the reactor and its surroundings, the glass may break. Besides suggesting the use of a metal reactor for the final prototype, it is also suggested to change the model in order to account for this effect. In addition, since the lab temperature curves were very inconclusive, one is not sure about validity of the consequent pressure values that were computed, as it was not found any additional information for making a possible comparison. By considering that glass may break under certain conditions, one might found out that the pressure generated might not even be enough to pump the desired amount of hydrogen towards the balloon. A compressor might be needed, which will increase the cost and complexity of the project, making it non-feasible. Finally, it is highly advised for one to correctly estimate the mass of all the prototype components: due to the pandemic, it was not possible to measure the majority of them and the space left for the reactants was highly affected.

Acknowledgements

The author would like to thank professors Alexandra Moutinho, Rui Neto, Aires dos Santos, José Pereira, Maria André, Viriato Semião, Eng. Luis Raposeiro and the author's family and friends.

References

[1] Michael Greshko. We discovered helium 150 years ago. are we running out? *National Geographic*, 2018.

[2] Google patented project loon. `https://www.youtube.com/watch?time_continue=1&v=jjSV_UAaO4I`.

[3] Andrey Sushko, Aria Tedjarati, Joan Creus-Costa, Sasha Maldonado, Kai Marshland, and Marco Pavone. Low cost, high endurance, altitude-controlled latex balloon for near-space research (valbal). In *2017 IEEE Aerospace Conference*, pages 1–9. IEEE, 2017.

[4] Luis Adriano Oliveira and António Gameiro Lopes. *Mecânica de Fluídos*. Lidel, 5th edition, 2016. ISBN: 978-989-752-221-5.

[5] Theodore L. Bergman Frank P. Incropera, David P. Dewitt and Adrienne S. Lavine. *Fundamentals of Heat and Mass Transfer*. John Wiley & Sons, 6th edition, 2007. ISBN: 978-0-471-45728-2.

[6] I. Muller and P. Strehlow. *Rubber and Rubber Balloons*. Springer, 2004. `https://d-nb.info/972144528/34`.

[7] Atmosphere model. `https://www.grc.nasa.gov/www/k-12/airplane/atmosmet.html`. Accessed: 2015-05-15.

[8] Weather balloons and accessories. `http://www.myhoskin.com/newsletters/PDF/WeatherBalloonsandAccessories.pdf`.